4-25-2019

Modeling Solitary Waves in the Earth's Magnetosphere

Jessica Thwaites
College of Saint Benedict/Saint John's University, JNTHWAITES@CSBSJU.EDU

Modeling Solitary Waves in the Earth's Magnetosphere

Jessica Thwaites

Mentor: Dr. Jim Crumley

College of Saint Benedict/Saint John's University

(Dated: May 2, 2019)

Solitary waves occur in many mediums, both on Earth and in space. These are nonlinear wave modes, which appear as single isolated wavelength or half wavelength of a linear wave. This study focuses on solitary waves observed in the Earth's magnetosphere, and used electric field data from NASA's Polar spacecraft, which took data in multiple regions within the magnetosphere. We developed a model in IDL for the shape of these waves, using a Gaussian function and performed statistical analysis on these waves to get a general idea of the shape of these solitary waves. The results of our model show a tight grouping of events in both width and amplitude. Events typically have a width with a value on the order of 105 and 106 1/s2, and amplitudes on the order of 10 to 100 V/m. These trends are expected, as the satellite flies through different parts of the wave depending on its direction and the solar wind conditions. These results give us a basis to analyze the shape of solitary waves in the Earths magnetosphere.

I. INTRODUCTION

Plasma makes up a large portion of the universe, possibly up to 99% of the matter in the universe, which includes stellar interiors and atmospheres, nebulae, and interstellar space [1]. Space is not empty; interstellar space is filled by plasma. Because plasma particles are charged, they have motion governed by magnetic fields in particular regions. Within our solar system, particles from the Sun that fill the interplanetary space is called the solar wind. Conditions of the solar wind and the Sun, as well as the influence of other magnetic fields in space, can cause many types of waves to be produced within the plasma.

Recent studies have shown an abundance of what are called *solitary waves*. These are nonlinear waves, which take the form of a single isolated half or full wavelength of a linear wave mode [1]. These electric field disturbances can be measured by satellites in multiple regions of the Earth's magnetosphere. This study takes data from NASA's Polar satellite, and aims to make a model of solitary wave data to analyze these waves in the magnetosphere.

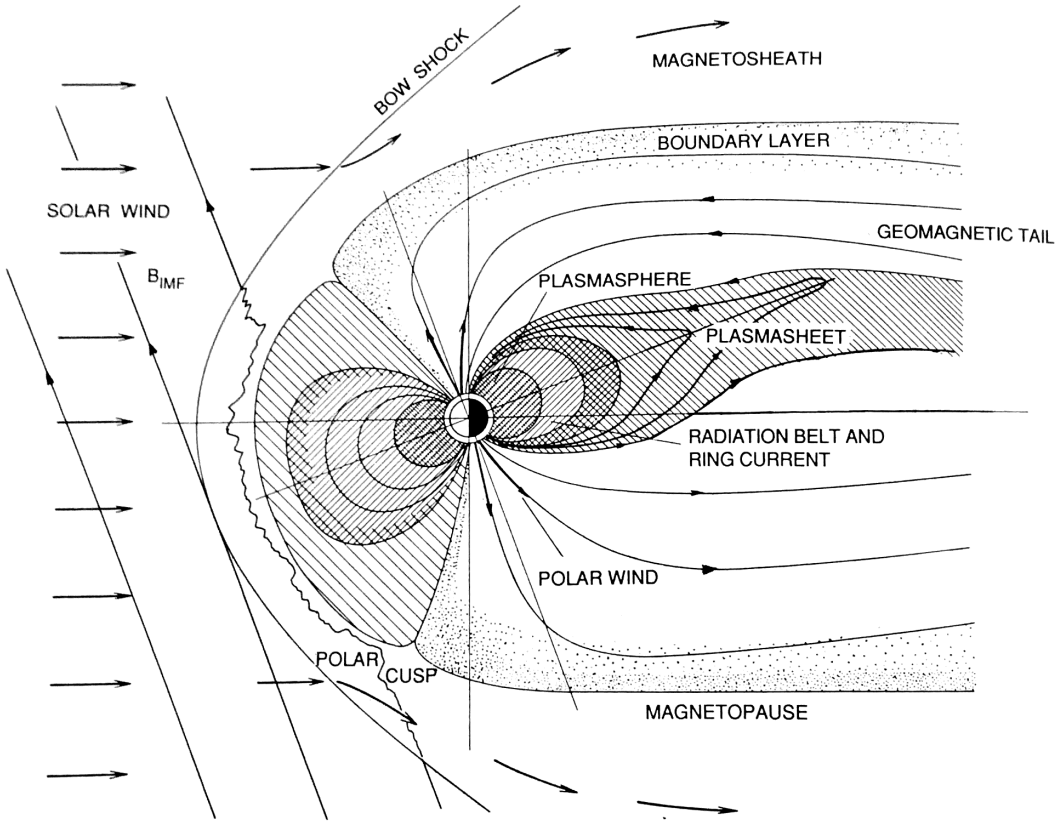

FIG. 1: Regions of the Earth's magnetosphere, from NASA [2]

A. Regions of the Earth's Magnetosphere

The Earth has several distinct regions within its magnetosphere. These regions are shown in Figure 1. In this figure, the Sun would be to the left, 1 AU away. The *solar wind* flows through interstellar space between the Earth and the Sun, and can be seen on the left side of this image. This solar wind is a part of the solar corona, which extends into space because the Sun's atmosphere is not in equilibrium [2]. Because this plasma is charged, these solar wind particles also include an *Interplanetary Magnetic Field* (IMF), which is an extension of the Sun's magnetic field.

Broadly, the *magnetosphere* is the region where Earth's magnetic field controls the motions of plasma particles [2]. In this paper, I will refer to the *dayside* and *nightside* of the Earth's magnetic field. These terms describe the parts of the Earth's magnetic field facing towards and away from the Sun, respectively. Thus, in Fig. 1, the central circle represents Earth, with the dayside illustrated by the unshaded half and the nightside by the shaded half of the circle. The region between them, where the Earth's field lines bend toward the poles of the Earth, is called the *cusp*.

The *bow shock* is the furthest region of interest, which is a collisionless shock wave that forms as the solar wind hits the Earth's magnetosphere [2]. This is, however, not technically part of the magnetosphere [3]. The outermost extent of the magnetosphere is the *magnetopause*, which under typical solar wind conditions is approximately 10 R_E from Earth. However, both the bow shock and the magnetopause locations are heavily dependent on solar wind conditions. On the nightside of the field, the *magnetotail* refers to the extended region of the Earth's magnetic field, which has been observed to extend beyond $200R_E$ [2].

Another important region shown in Fig. 1 is the *plasmasphere*, which is essentially a reservoir of plasma that alternately fills and drains, depending on solar wind conditions [4]. This region contains the *ionosphere*, which is a permanent population of ionized atmosphere. The ionosphere typically extends to about 1000 km (1.2 R_E) above the Earth's surface [3].

B. Solitary Waves

Historically, solitary waves have been studied as a type of nonlinear plasma wave. Studying solitary waves allows us to study the evolution of interacting plasma waves through interstellar space [5].

Solitary waves are unique because of some of their properties. In the period 1970-1982 many experiments on solitary waves in plasma were conducted [5]. Simulations were run which showed that after a collision, solitary waves retain their shape [5]. The effects of dissipation of solitary wave energies have a large impact in plasma physics, as was studied by Ott and Sudan in 1969 [5].

These studies have provided some examples of the properties of solitary waves. We aim to expand upon that basis by modeling the shape of solitary waves.

C. Polar Satellite

NASA operated the Polar satellite, which was launched in 1996 in a highly elliptical orbit at an 86 degree inclination with a period of about 17.5 hours [6]. The goal of the satellite was to observe the magnetosphere around the cusp and ionsphere. Polar's orbit can be seen in Fig. 2a. This figure shows the orbit of Polar with some of the Earth's magnetic field lines superimposed.

Because of its highly elliptical orbit, Polar was able to sample data in many regions of the magnetosphere, including the magnetosheath, cusp, and bow shock. This allows us to get a sample of solitary wave data from different regions within the magnetosphere. Polar took data for many

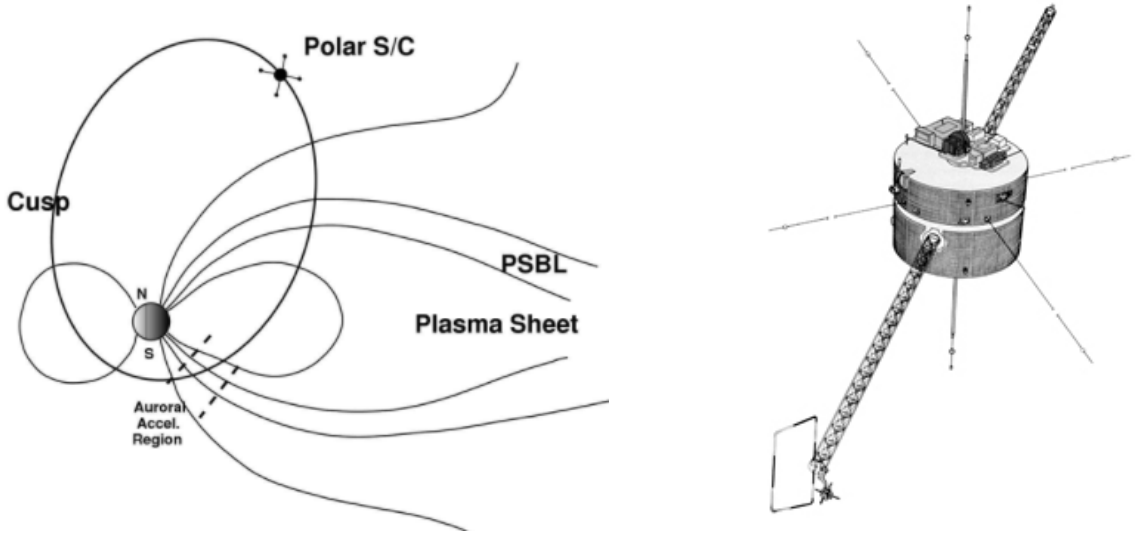

(a) Orbit of Polar around the cusp region.

(b) Illustration of NASA's Polar Satellite

FIG. 2: Polar had a highly elliptical orbit that passed through multiple regions of the magnetosphere. Here, the plasma sheath boundary layer (PSBL) and the plasma sheet are shown on the diagram to illustrate the regions of the Earth's ionosphere through which Polar passed [6].

years in the cusp. Each year it changed some of its settings, allowing the data to be used in multiple experiments. In 1997, Polar took data with settings most conducive to finding solitary waves. In particular, our study uses data from the Electric Fields Instrument (EFI) on Polar collected in 1997[6].

II. THEORY

A. Magnetosphere Plasma Physics

Plasmas can be defined as an electrified gas that is dissociated into positive and negative ions that exhibit collective behavior [1]. In uncharged gas, motion is determined by collisions with other molecules. However, because plasma is charged, plasma particles are governed by the Lorentz force, given by [4]:

$$m\frac{d\vec{v}}{dt} = q(\vec{E} + \vec{v} \times \vec{B}) \tag{1}$$

The motion of these charged particles gives rise to electric and magnetic fields, which affects the motion of other plasma particles at a distance away [1]. External magnetic fields, such as the Earth's magnetic field, cause the charged plasma particles to gyrate around magnetic field lines at

the cyclotron frequency, ω_c:

$$\omega_c = \frac{qB}{mc} \tag{2}$$

With q as the charge of the particle (ion or electron), B the magnitude of the magnetic field, m the mass of the particle, and c the speed of light. The motion of a charged particle in the Earth's magnetic field can be seen in Fig. 3.

In some cases, we can approximate a plasma as a fluid, which allows us to analyze the collective behavior of the plasma [1]. This adaptation of classical fluid dynamics to plasmas leads to the derivation of *magnetohydrodynamics* (MHD) [4]. MHD is "a branch of continuum mechanics that deals with the motion of electrically conducting material in the presence of electromagnetic fields" [2]. It ignores the independent motion of particles and describes the fluid as a whole.

This fluid could be approximated using a dielectric constant, valid when the frequency is low and the motion is transverse to the magnetic field [1]:

$$\epsilon = 1 + \frac{4\pi\rho c^2}{B^2} \tag{3}$$

Then, if we only include ions and electrons in the plasma, we can write the charge and current densities as [1]:

$$\sigma = n_i q_i + n_e q_e \tag{4}$$

$$\vec{j} = n_i q_i \vec{v_i} + n_e q_e \vec{v_e} \tag{5}$$

Which makes the set of Maxwell's equations for our approximation [1]:

$$\begin{aligned} \vec{\nabla} \cdot \vec{E} &= 4\pi(n_i q_i + n_e q_e) & \vec{\nabla} \times \vec{E} &= -\dot{\vec{B}} \\ \vec{\nabla} \cdot \vec{B} &= 0 & c^2 \vec{\nabla} \times \vec{B} &= 4\pi(n_i q_i \vec{v_i} + n_e q_e \vec{v_e}) + \dot{\vec{E}} \end{aligned} \tag{6}$$

And the combination of pressure-gradient force and Lorentz force becomes [1]:

$$m_i n_i [\frac{\partial \vec{v_i}}{\partial t} + (\vec{v_i} \cdot \vec{\nabla})\vec{v_i}] = q_i n_i (\vec{E} + \vec{v_i} \times \vec{B}) - \vec{\nabla} p_i \tag{7}$$

$$m_e n_e [\frac{\partial \vec{v_e}}{\partial t} + (\vec{v_e} \cdot \vec{\nabla})\vec{v_e}] = q_e n_e (\vec{E} + \vec{v_e} \times \vec{B}) - \vec{\nabla} p_e \tag{8}$$

With p as the pressure, defined as $p = nkT$, because equilibrium plasma behaves like an ideal gas. Then n_i, n_e are the number of ion and electron particles per cm^3 respectively [2]. We also have two equations of continuity for each species [1]:

$$\begin{aligned} \frac{\partial n_i}{\partial t} + \vec{\nabla} \cdot (n_i \vec{v_i}) = 0 \\ \frac{\partial n_e}{\partial t} + \vec{\nabla} \cdot (n_e \vec{v_e}) = 0 \end{aligned} \tag{9}$$

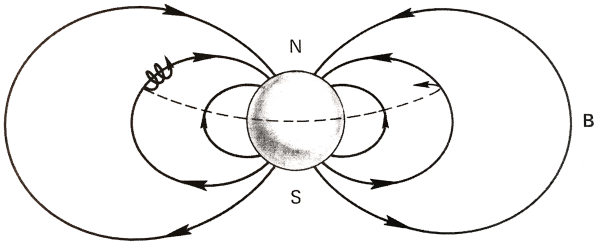

FIG. 3: Motion of a charged particle trapped within Earth's magnetic field. Cyclotron motion perpendicular to Earth's field can be seen, as well as orbit around the Earth. [1]

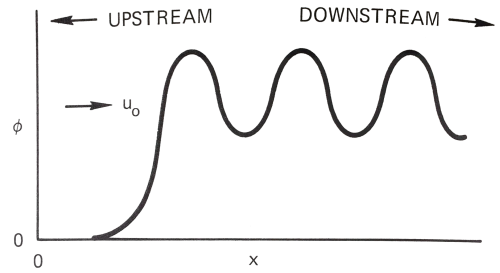

FIG. 4: A typical potential distribution in an ion acoustic shock wave. The vertical axis shows the scalar potential and the horizontal axis is a length variable. This wave moves to the left with a velocity given by u_0 [1]

We also have a thermodynamic relation relating the pressure p to n via the adiabatic exponent, $\gamma = C_p/C_v$ with C_p and C_v as the specific heat at constant pressure and volume respectively [4]:

$$\frac{d}{dt}(p\rho^{-\gamma}) = 0 \tag{10}$$

This set of equations 6 to 10 governs the motion of particles within this fluid plasma approximation [1]. These equations show that even in the absence of collisions waves can still travel in space, through ions transmitting vibrations via electric and magnetic fields [1].

B. Waves in Plasma

There are many types of waves in space, which can be generated by the Sun, solar wind interactions, shocks, magnetospheres, or ionospheres [2]. The solar wind can cause pressure disturbances and waves at the magnetosphere, due to fluctuations in solar wind density [4]. The Sun can produce changes in the solar wind, which rapidly compresses the magnetosphere. One major example of this would be in the formation of Coronal Mass Ejections (CMEs), which is a large quantity of plasma that is ejected from the surface of the Sun [4].

These waves depend on plasma parameters, and can be described with reference to $\vec{k}$, the propagation vector, and $\vec{E}$, the electric field [2]. When these waves are found in regions where MHD theory describes the plasma, they are called MHD waves, which are low-frequency waves (Low frequency means that their frequency is lower than the ion Larmor frequency) [2]. MHD

waves are defined as *electrostatic* if $\vec{k}$ is parallel to $\vec{E}$, and *electromagnetic* if $\vec{k}$ is perpendicular to $\vec{E}$ [2]. These waves can propagate along the magnetic field direction [2].

A particular type of waves in space plasmas are called *ion acoustic waves*. If we consider the ion motions in the plasma, then sound waves are generated through interaction between plasma particles by means of their charge [2]. We expect electric field to be of the form [2]:

$$\vec{E} = -\vec{\nabla}\phi \tag{11}$$

The ion fluid equation (Eq. 7) without an ambient magnetic field then becomes [2]:

$$m_i n_i [\frac{\partial \vec{v_i}}{\partial t} + (\vec{v_i} \cdot \vec{\nabla})\vec{v_i}] = q_i n_i \vec{E} - \vec{\nabla} p_i \tag{12}$$

The right side of this equation can be rewritten using $p_i = \gamma_i n_i k T_i$ and Eq. 11 to give [2]:

$$q_i n_i \vec{E} - \vec{\nabla} = -q_i n_i \vec{\nabla}\phi - \gamma_i k T_i \vec{\nabla} n_i \tag{13}$$

Recognizing that electrons have a thermal energy kT_e, these electrons must be distributed according to a Maxwellian distribution [2]:

$$n_e = n_0 \exp[\frac{e\phi}{kT_e}] \tag{14}$$

Which gives a phase velocity of the ion acoustic waves of:

$$\frac{\omega}{|\vec{k}|} = [\frac{k_B T_e}{m_i(1 + \vec{k}^2 \lambda_D^2)}]^{1/2} \tag{15}$$

With λ_D as the Debye length and assuming $T_i << T_e$, which is the conditions of the solar wind. This phase velocity is equal to the group velocity for ion acoustic waves. These ion acoustic waves are essentially constant velocity waves, which require thermal motion of particles.

C. Solitary Waves

Solitary waves can develop from ion acoustic waves, which are pressure pulses travelling in a fluid [2]. Solitary waves appear as single, isolated half or full wavelengths of a linear wave mode. These waves are "observed as a depletion or increase of the plasma density that also coincides with a change in the electrostatic potential" [7].

These waves follow what is called the Sagdeev potential, which can be seen in Fig. 6. Starting with Poisson's equation [7]:

$$\frac{\partial^2 \phi}{\partial x^2} = 4\pi e(n_0 e^{e\phi/kT_e} - n_i) \tag{16}$$

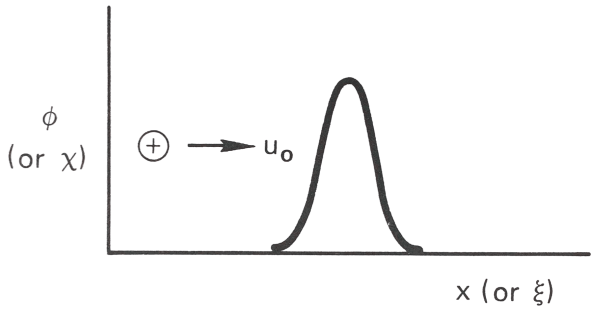

FIG. 5: The potential of a solitary wave moving to the left. The axes show the electric potential with respect to displacement of a pulse traveling to the right at velocity u_0 [1].

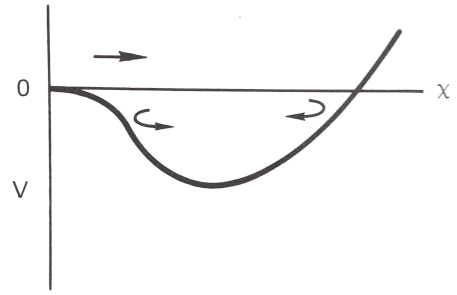

FIG. 6: The Sagdeev potential, $V(\chi)$, which shows the potential well, with the lower arrows describing a particle that is trapped within the well [1].

Then including the continuity equations and integrating, we can get a differential equation [7]:

$$(\frac{\partial\phi}{\partial x})^2 = 8\pi n_0(um_i\sqrt{u^2 - \frac{2e\phi}{m_i}} + kT_e e^{e\phi/kT_e} - m_i u^2 - kT_e) \tag{17}$$

Which has the form of a potential equation:

$$\frac{1}{2}(\frac{\partial\phi}{\partial x})^2 + U(\phi) = 0 \tag{18}$$

With $U(\phi)$ being the Sagdeev potential.

The ion acoustic soliton solution to this potential is given by

$$\phi = \frac{3z}{c_s}\text{sech}^2(\sqrt{\frac{z}{2c_s}}(\frac{x-ut}{\lambda_D}) \tag{19}$$

With c_s as the acoustic speed, u the wave speed, x the coordinate in the direction of propagation, and the dimensionless quantity $z = \frac{u}{c_s} - 1$ [7].

This study focuses on solitary wave pulses, which take the form of density changes in the plasma at the magnetosphere, and thus correspond to changes in the electrostatic potential. This is expected to follow the Sagdeev potential, as outlined above. We believe the solitary waves we are seeing in our data may be ion acoustic solitons. These appear to have the shape given in Fig. 5, which appears to be an isolated half wavelength of a linear wave mode.

III. DATA COLLECTION: POLAR SATELLITE

The data from Polar is in the form of electric field versus time, with electric field having 3 components: one parallel to Earth's field and two perpendicular components. We expect the

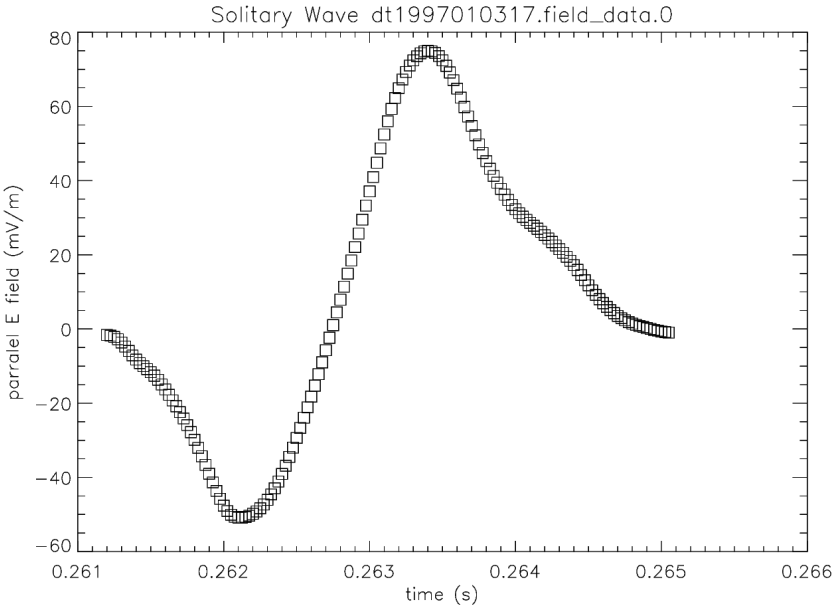

FIG. 7: Scatterplot of solitary wave data from Polar, produced in IDL

solitary wave to follow the Earth's magnetic field lines [7] and thus to appear primarily in the component of electric field parallel to that of the Earth. For this reason, we extracted the parallel component of the electric field data and plotted this with respect to time. A scatterplot example of this electric field data can be seen in Fig. 7.

This data appears to have the general shape of the derivative of a Gaussian function. We expect the electric field to be the gradient of the electric potential according to Equation 11, and thus the potential function would be that of a Gaussian. This potential can be seen in Fig. 5, which appears to have a Gaussian shape. This informed our choice of model function used in IDL.

IV. DEVELOPMENT OF A MODEL FOR SOLITARY WAVES

The purpose of this study is to develop a working shape model for solitary waves. Our code attempts to model these nonlinear wave modes by applying a derivative of a Gaussian fit function to the waves. A Gaussian shape was chosen due to a visual resemblance to the shape of the derivative of a Gaussian function.

A. Choice of Coding Language

Initially, this model was made in Mathematica, which used the `NonlinearModelFit` function built into the Mathematica language. In doing this, we tried two shapes to model the waves: a sine function and a Gaussian. The sine function did not produce good fit results in Mathematica. This may have been because of the periodicity of a sine wave, as solitary waves are by definition a single isolated wave pulse. Using Mathematica prompted some limitations. Many of our events were unable to be fit to our functional form with the Mathematica process. This happened most often for events that visually did not appear to perfectly follow the expected Gaussian derivative function. It was also more difficult to manipulate the fit function in Mathematica. The command itself, `NonlinearModelFit`, takes the form:

$$\texttt{NonlinearModelFit[data, form, \{}\beta_1\texttt{, ...\}, \{}x_1\texttt{, ...\}]}$$

With x_i giving the data array, `form` giving the full functional form, β_i giving parameters for the program to solve, and x_i giving the variables contained in the function. We were unsure the method being used by the program to choose the parameters (β_i).

B. IDL Model

Because of these limitations we found in using Mathematica, the decision was made to switch languages and use the Interactive Data Language (IDL). We kept the Gaussian model developed in the Mathematica code, which gave us more reliable results for the fits than the sine function, but changed languages. We hoped this approach would give more reliable results without relying on perfect cases. Using IDL, we are able to fit 158 data sets.

1. CurveFit

`CurveFit` is a built-in function to IDL that produces a non-linear fit given input of a functional form and its partial derivatives [8]. It takes the form:

$$\texttt{fit = CURVEFIT(}X_i\texttt{, }Y_i\texttt{, parameters, SIGMA, FUNCTION\_NAME= 'name')}$$

With the inputs of X_i and Y_i being the dependent and independent variables, respectively, to which the program will fit. The array, `parameters` is a constant array that will hold the values for the four fit parameters found by IDL. These must be initialized close to the expected values, but

must not be greater than the value the program will find. The `SIGMA` is also an array, with the same dimension as the `parameters` array. It gives the standard deviation of each parameter as is found by the function during the fitting process.

The `FUNCTION_NAME='name'` gives a path to a *.pro* file which contains the functional form.

We chose to have 4 parameters in the code for the model. This model takes the form of the derivative of a Gaussian function:

$$f(x) = a_0(x - a_2) * e^{a_1(x-a_2)^2} + a_3 \tag{20}$$

With a_0 proportional to the amplitude of the wave, a_1 proportional to the width of the wave, a_2 as the horizontal displacement from $t = 0$, and a_3 as the vertical displacement from $E_{parallel} = 0$. Then a_0 has units of mV/(m*s), vertical offset a_3 has units of mV/m, a_1 has units of inverse time squared ($1/s^2$), and the horizontal displacement a_2 has units of time (s).

However, we want these parameters to have units that make physical sense, so we can recast this function so that the a_0 and a_1 are the amplitude (in mV/m) and width (in s) of the wave. Doing this, with b as the amplitude in mV/m and c as the width in s, we can write our fit function as:

$$f(x) = \frac{b}{c}(\frac{x}{c} - \frac{a_2}{c}) * e^{0.5(\frac{x}{c} - \frac{a_2}{c})^2} + a_3 \tag{21}$$

With

$$b = \frac{a_0}{2a_1} \qquad\qquad c = \sqrt{\frac{1}{2a_1}} \tag{22}$$

Integrating this shows the Gaussian form of the potential that is expected:

$$F(x) = b * e^{0.5(\frac{x}{c} - \frac{a_2}{c})^2} \tag{23}$$

We also analyzed the full width at half maximum (FWHM) for our events, which is given by the equation:

$$\text{FWHM} = 2\sqrt{2\ln 2} * c \tag{24}$$

These parameters give us inherent characteristics about the waves themselves, and will be analyzed to show a distribution of waves observed by the satellite. The same scatterplot from Fig. 7 but with the specific parameter values (b/c, c, a_2, a_3) for that wave can be seen in Fig. 8.

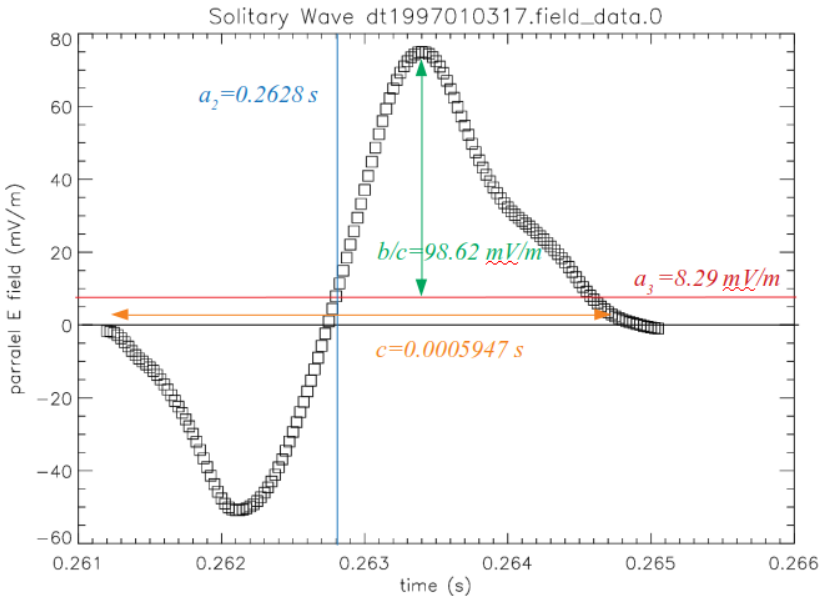

FIG. 8: Scatterplot of solitary wave data, with overlay showing the parameter values for that particular wave.

2. *Parameters*

One of the requirements in both Mathematica and IDL was that the languages need to have the parameter array initialized with a "guess" for the parameter values. This helps to avoid the fit program getting locked in a local minimum for each of the parameters, rather than the best fit values. However, developing the theory for what these initial guesses need to be was more involved than initially thought. One of the limitations that we discovered was that the initial parameter value guesses supplied in IDL need to be lower than the actual value.

The displacement parameters a_2 and a_3 were the most straightforward to find. The horizontal displacement a_2 was the only parameter that is truly arbitrary in our theory. The time that the wave began or ended is irrelevant to the actual shape of the wave itself. Since each parameter must be lower than its actual value, and a Gaussian is normally centered around 0, the time value of the first data point will always be less than the horizontal displacement, so this became the initial guess for this parameter. The blue line in Fig. 8 shows this horizontal displacement from 0.

The vertical displacement, a_3, is more theoretically significant; theoretically, this parameter would have a value that shows a voltage drop caused by the wave. However, in our code it really acts as a "fudge factor" because often the positive and negative amplitudes were significantly different. This voltage offset is relatively small in all of our data, so the initial guess for a_3 was set

to 0.

The width-like parameter a_1 should be related to the width of the wave. This can be described by the equation:

$$a_1 = \frac{1}{2c^2} \tag{25}$$

Where c, the width, can be approximated directly by our code.

The amplitude-like parameter, a_0, was the most difficult to calculate directly. We had difficulty finding a theoretical way to model this parameter, and thus in the guess we simply set it to 10000, which was smaller than most of the amplitude values found by IDL for each individual event and gave us the most consistent results.

These values for all 4 parameters should give us a distribution of the wave data, which can be analyzed to determine the average size and shape of our solitary waves. Although IDL gave us better results than the code in Mathematica, there were still some limitations, which led to us being unable to fit 25 of our 183 events. Adapting the model to fit these last few cases would allow us to improve the model accuracy but would require further research.

V. ANALYSIS

A. Size Distributions of Solitary Wave Events

The observed width and amplitude can be analyzed to get a general idea of the 3-dimensional shape of the waves as they pass the spacecraft. The waves themselves travel parallel to the Earth's magnetic field, but the satellite could be oriented in any direction relative to this field. If the satellite does not fly directly through the center of a wave, but catches only the side or most extreme edge of the wave, we expect the amplitude and width reported by the satellite to be less than the amplitude and width of the center of the wave packet. For this reason, we expect to see an approximately normal distribution in sizes and shapes of the waves, which when analyzed together should give us an idea of the typical solitary wave shape as it travels through the magnetosphere. A histogram of amplitude values can be seen in Fig. 9a and a histogram of width values can be seen in Fig. 9b.

The histograms of width and amplitude parameters allow us to consider these two parameters separately. The amplitude histogram appears to have an even spread, leading us to believe that it could possibly follow a normal distribution, which would be consistent with our theory. However, there are some alternative explanations to the distribution of events. Low amplitude events could

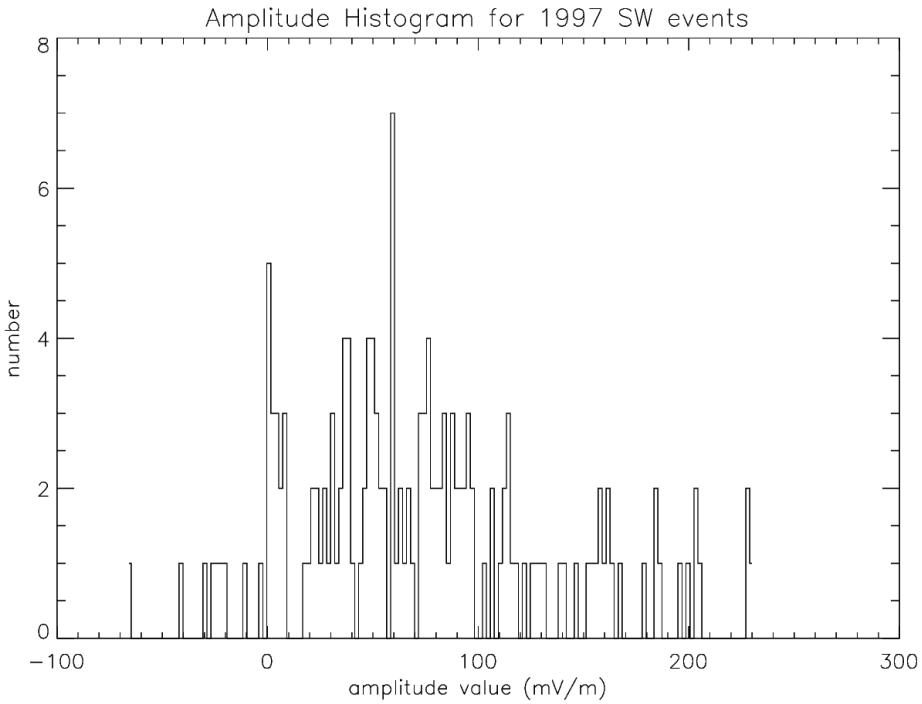

(a) Histogram of values found by the program for the amplitude parameter, b, in units of mV/m.

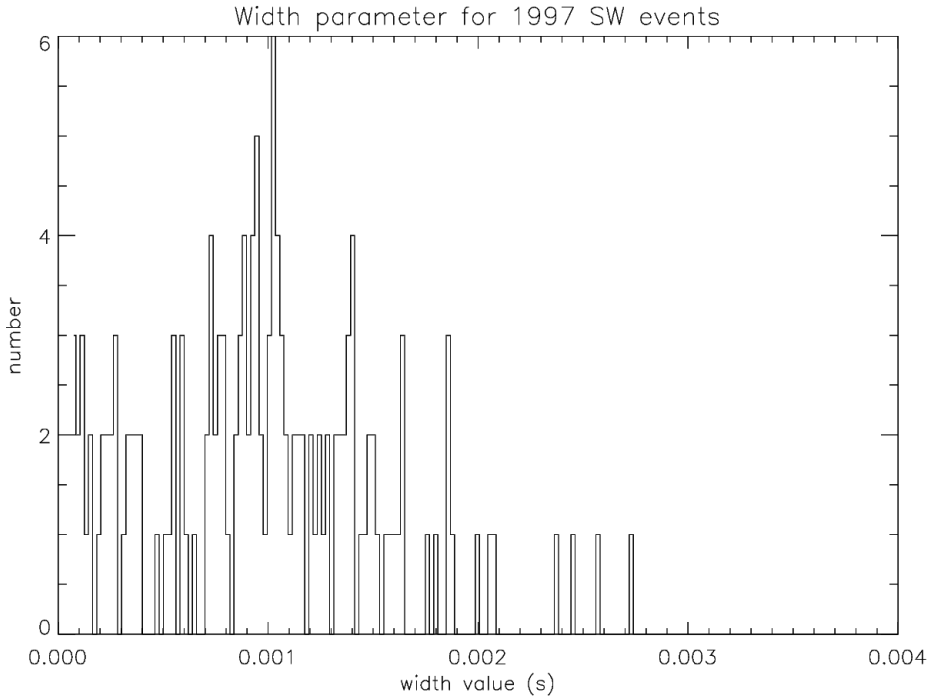

(b) Histogram of width parameter values found by the program, c, in units of s.

FIG. 9: Histograms of amplitude and width parameters found by our shape fitting code. Plots made using IDL.

become lost in the background electric field fluctuations and thus some small amplitude events could be missing from our data set. As the amplitude increases, the wave could take on a different shape depending on the conditions of the solar wind and ionosphere that particular day, which could also cause the spread seen in our data. There are also some negative amplitude values; these represent waves that were travelling in an opposing direction to the majority of the events. These are waves that are reflected from the Earth's magnetosphere, rather than moving downward as expected in most ion solitary waves.

In the width histogram, the sharp width peak appears in the low width values. This could mean that most solitary waves picked up by the satellite happen on a very short time scale, which makes sense because they are a single isolated wave pulse. However, it could also stem from a more mechanical source; our code worked more consistently with the waves that had a lower width value, and several of the 25 cases that the code was unable to fit were much slower pulses. There are also 3 points with much higher with values not shown on this plot which appear to be outliers. These were removed in order to show the majority of the width values more clearly.

There is an additional source of error that may be present in these plots. Our theory is consistent for ion solitary waves, not electron solitary waves, which move more quickly and in the opposite direction [7]. However, these two types appear similar in our data, so some electron solitary waves may be present in our data which could affect the shape of the histograms.

In the future, applying this code to more events would enable us to eliminate some of the error from these histograms. Re-working some of the code to could also change the shape of the width graph, as we are able to incorporate some of the most slowly moving waves.

B. Width versus amplitude

Solar wind and ionosphere conditions could impact the size and shape of solitary waves seen by Polar. If this is true, then the width and amplitude should be correlated and would depend on the solar wind conditions. However, in 10a, we see a broad range of width values corresponding to very consistent amplitude values. This suggests that solar wind conditions may impact the solitary waves' width, but the amplitude remains very tightly peaked. There are a few outliers which have much higher amplitude than the bulk of our events. These may be outliers from our code, and could represent less precise fits, or be electron instead of ion solitary waves. The width could be dependent on the relative velocity of the spacecraft to the wave, which could also explain the greater variation in observed width.

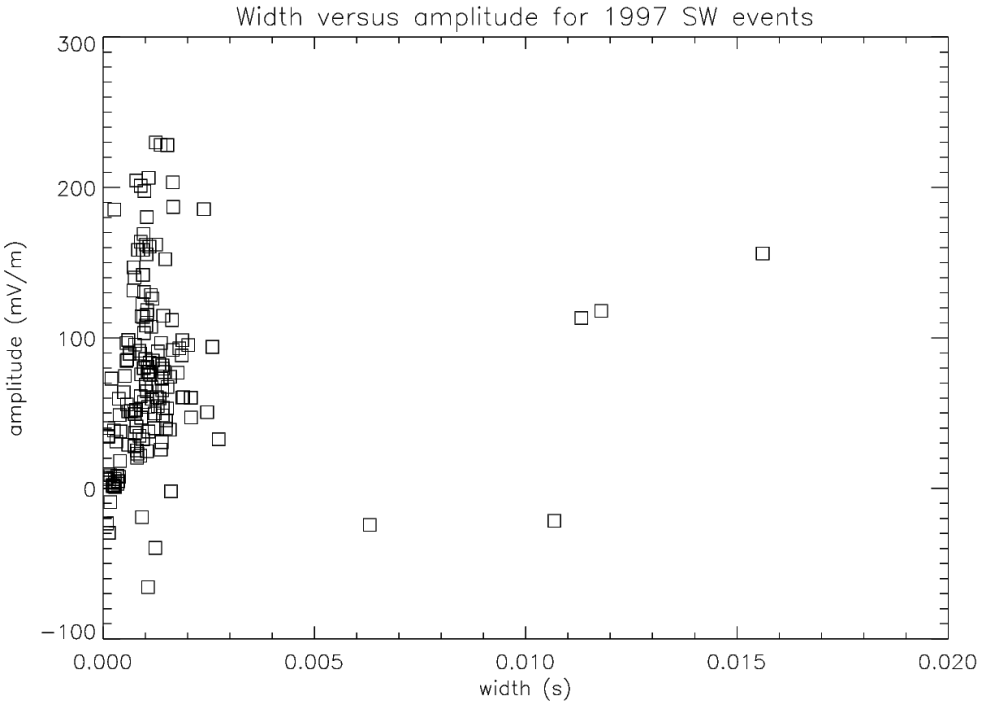

(a) Scatterplot of width and amplitude parameter values for solitary wave events.

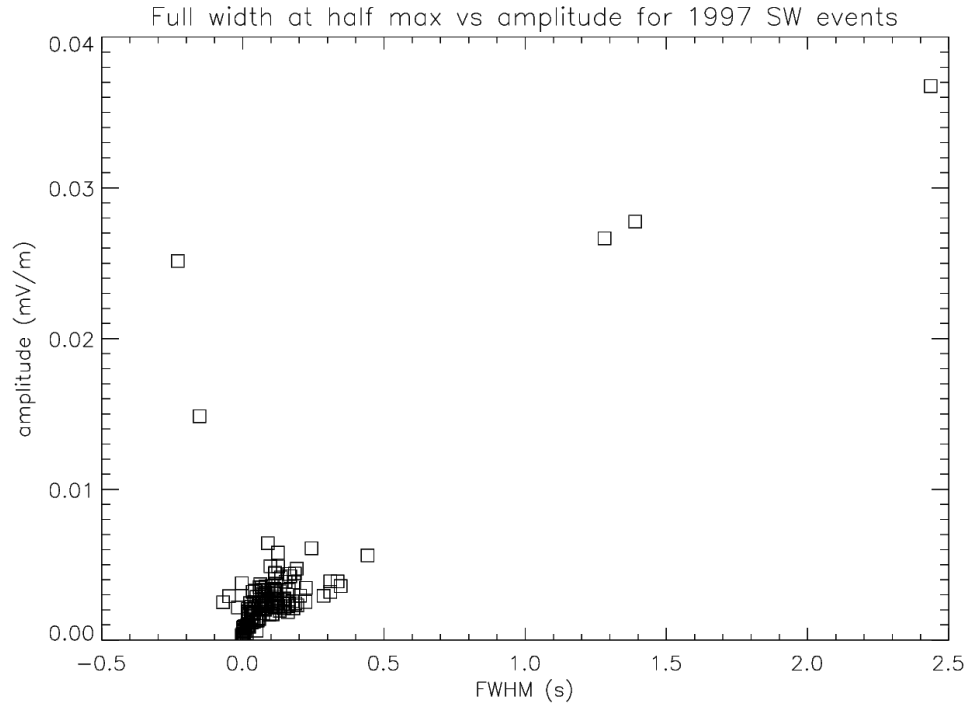

(b) Scatterplot of full width at half max values and amplitude parameters.

FIG. 10: Plots of amplitude parameters versus width parameters for corresponding events found by our shape fitting code. Plots made using IDL.

The amplitude versus the full width at half maximum also shows a tight grouping of values of FWHM and amplitude values. The FWHM allows us to have another width-dependent value to compare. Here it appears that there is a tight grouping of values for FWHM and amplitude values, with a few outliers far removed from a majority of points. In the future, this plot could provide a good jumping-off point to analyzing more events and finding a consistent trend between the width and amplitude of these events. This could potentially take the form of a linear or power-law fit.

VI. CONCLUSIONS

In conclusion, we were able to develop a shape model in IDL to fit solitary wave events. This model converged on values for all but 25 out of 183 of our solitary wave events. This shows that for our data, even the waves that did not visually appear to fit the derivative of a Gaussian model, the code was able to find solutions for these cases. This model developed included 4 parameters: amplitude, width, and vertical and horizontal offsets. This study focused on the values found for event amplitude and width.

Our analysis shows the general shape of our solitary wave events. Both the amplitude and width values found by our code for these events appears to be peaked in a mostly normal distribution. This is to be expected in our theory as the satellite passes through different parts of the wave depending on direction the satellite is flying and solar wind conditions change depending on the day. Our data shows a tight grouping of the width and amplitude of these wave events. Further analysis could show a trend in these values.

VII. FUTURE WORK

This project provides a possible basis for work that could be continued to develop a complete model for the shape of these solitary waves. The code still is unable to fit 25 cases, many of which appear to visually have the shape of a Gaussian function and do not appear to be anomalous. However, their duration was significantly longer than the other cases, which affected the width parameter in the code. With the recasted function, given by eqn. 21, we may be able to estimate a_0 in a manner that is more accurate and efficient. If we are able to do this, many of the events with parameters that had larger variations from our initial estimates could be fitted by our function, leading to a better success rate for our program.

This project could also be adapted to fit anomalous events that do not appear to be a Gaussian

shape, but did work with our code. These events may have occurred if the satellite flew through only part of a wave, or an extreme edge. These could be the outliers seen in the width versus amplitude plots (Fig. 10).

Once these adaptations are made, it would be very interesting to analyze the vertical displacement parameter. This parameter, if significant and nonzero, would show a small potential drop over the wave, which would be an interesting phenomenon to study for these waves. It was decided not to focus on this in this study, because for many of the events a more accurate shape representation of the wave events would be needed to determine if this parameter is significant and represents a characteristic in our data, or if it should be attributed to experimental error.

Another method that could be used to check the veracity of the parameters found by our code would be to compare these parameters to the amplitude and width of the waves as found by another program, called *delaytime*. This program was run through Polar's data to isolate solitary wave events for use in this study, and also found estimates for both amplitude and width. In the future, comparing these values would allow us to check the values found by our IDL code.

VIII. ACKNOWLEDGEMENTS

This work was begun as part of the CSB/SJU MapCores Research program. The author would like to acknowledge Dr. Jim Crumley for all his help over the course of the semester. The author would also like to acknowledge NASA and the creators of EFI on Polar for the data used in this study.

---

[1] F. F. Chen, *Introduction to plasma physics and controlled fusion*. 1984.

[2] G. K. Parks, *Physics of space plasmas: an introduction*. Boulder, Colo.: Westview Press, 2nd ed. ed., 2004.

[3] J. Crumley, "Magnetopause Lab," in *PHYS 370: Advanced Physics Lab Manual*, Jan. 2019.

[4] C. T. Russell, J. G. Luhmann, and R. J. Strangeway, *Space Physics: An Introduction*. Cambridge ;: Cambridge University Press, 2016.

[5] D. F. Escande, "Contributions of plasma physics to chaos and nonlinear dynamics," *Plasma Physics and Controlled Fusion*, vol. 58, p. 113001, Nov. 2016.

[6] A. Szabo, "NASA Polar Project," Jan. 2017.

[7] J. P. Crumley, *Particle Simulations and Polar Spacecraft Observations of Solitary Waves in the Magnetosphere*. PhD thesis, University of Minnesota, Twin Cities, 2002.

[8] K. P. Bowman, *An introduction to programming with IDL: Interactive Data Language*. Amsterdam ;: Elsevier Academic Press, 2006.